Dissociation Conditions of Methane Hydrate in Mesoporous Silica Gels in Wide Ranges of Pressure and Water Content

Eugeny Ya. Aladko,[‡] Yury A. Dyadin,[†,‡] Vladimir B. Fenelonov,[§] Eduard G. Larionov,[‡] Maxim S. Mel'gunov,[§] Andrej Yu. Manakov,*[,‡] Anatoly N. Nesterov,[||] and Fridrikh V. Zhurko[‡]

Nikolaev Institute of Inorganic Chemistry SB RAS, 3 Prospekt Akad. Lavrentieva, Novosibirsk, 630090, Russian Federation, Boreskov Institute of Catalysis SB RAS, 5 Prospekt Akad. Lavrentieva, Novosibirsk, 630090, Russian Federation, and Institute of Earth Cryosphere SB RAS, 86, Malygina str., Tyumen, 625026, Russian Federation

Received: April 13, 2004; In Final Form: July 30, 2004

The temperature of methane hydrate dissociation in silica mesopores has been monitored within a wide range of pressures from 10 MPa to 1 GPa. Because the determination of pore size appears to be crucial for the studied phenomenon, several methods of calculation have been applied. According to our findings, the size that corresponds to the mean size of the most representative pores is to be considered as the most reliable. It was concluded that the shape of hydrate particles replicates a host space of pores and may have a complex (e.g., fractal) shape. An attempt to simulate the curvature of hydrate particles by globular (quasi-spherical), elongated (quasi-cylindrical), or any intermediate models has been done. The quasi-spherical model seems to be more adequate for hydrate particles in small pores (<8 nm), while the quasi-cylindrical model fits better the experimental data for hydrate particles in larger pores. According to our experimental results, the hydrate can be formed in pores only by capillary condensate, without involving the water layers tightly bound by the surface, and pressure has an insignificant effect on the decrease of the dissociation temperature of the confined hydrate. A new effect of the formation of hydrates at a temperature higher than the bulk hydrate dissociation temperature has been observed for silica gels with the narrowest pores studied.

Introduction

Recent interest in gas hydrates is caused by the discovery of large deposits of natural gas in a hydrate form.[1] To the best of our knowledge, natural gas hydrates bed mainly in marine shelves and the great oceans; because they are disseminated under high pressures in the pores of coarse- and fine-grained deposits, only about 6% of their total amount are contained in a bulk form.[2−4] Equilibrium dissociation pressures of hydrates and their thermodynamic properties are known to depend on the size of "host" pores. In coarse-grained systems (sand rocks), the dissociation temperatures of hydrates are practically identical to those of bulk hydrates.[5] In fine-porous media, the activity of water is changed due to interaction with the surface of the host porous material that results in a decrease of the dissociation temperature of the hydrates.[6−14]

Two main approaches have been used to describe this phenomenon, both based on the classical theory of capillary effects. The effect of fine-porous medium on the stability of a confined methane hydrate has been taken into account[9,10] by the correction of the classical statistical-thermodynamic model of van der Waals and Platteeuw[15] for thermodynamic activity of water in pores. The value of specific interfacial energy at the water−hydrate interface appears to be close to that on the water−ice interface (0.029 and 0.0267 J/m^2 in refs 9 and 10, respectively). Both values provide a fairly good agreement between the calculated and experimental data that were available at that time. According to another approach,[11−14] the measured dissociation temperature of gas hydrates in fine-porous glasses and silica gels can be considered in terms of the Gibbs−Thomson equation:[16]

$$\frac{\Delta T(d)}{T_{\text{bulk}}} = -K\frac{1}{d} \tag{1}$$

where

$$K = \frac{a\gamma_{\text{hw}}}{\rho_{\text{h}} L_{\text{h}}} \tag{2}$$

Here, $\Delta T(d)$ is the decrease of the temperature of the phase transition as a function of the pore diameter d, T_{bulk} is the temperature of the phase transition in a bulk phase, ρ_{h} is the density of the hydrate, γ_{hw} is the specific interfacial energy on a liquid−hydrate interface, and L_{h} is a latent heat of hydrate dissociation. The value of a is a function of the surface curvature of gas hydrate particles and in the simplest case is given by the equation for the solid−liquid interface curvature K_{m}, which may be determined as:

$$a = 2K_{\text{m}}; \quad K_{\text{m}} = \frac{1}{R_{\text{m}}} = \frac{1}{2}\left(\frac{1}{R_1} + \frac{1}{R_2}\right) = \frac{R_1 + R_2}{2R_1R_2} \tag{3}$$

where R_{m} is the mean radius of surface curvature, R_1 and R_2 are the principal radii of curvature ($R_1 = R_2$ for spherical particles, $R_2 = \infty$ for cylindrical particles, etc.). These equations imply that when d is the typical pore diameter, a is equal to 4

* To whom correspondence should be addressed. Telephone: (7-3832) 39-13-46. Fax: (7-3832) 34-44-89. E-mail: manakov@che.nsk.su.
† Deceased.
‡ Nikolaev Institute of Inorganic Chemistry.
§ Boreskov Institute of Catalysis.
|| Institute of Earth Cryosphere.

10.1021/jp048389q CCC: $27.50
Published on Web 09/29/2004

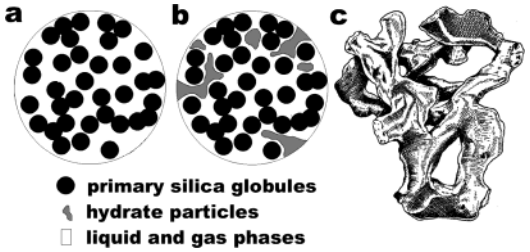

Figure 1. (a) Schematic representation of the silica gel texture; (b) silica gel with confined particles of gas hydrate; and (c) shape of the large cluster of gas hydrate particles which may form in porous space (reproduced from ref 17).

and 2 when hydrate particles are modeled as spherical[11,12] or cylindrical[13,14] particles, respectively.

Both approaches discussed above are related to a problem of correct determination of the typical pore size. The real structure of silica gel is formedvia random packing of primary spherical globules (Figure 1). Thus, the pore space of silica gel and other similar disordered structured materials may be assumed as a three-dimensional labyrinth of interconnected pores of different shapes and sizes. This labyrinth contains expansions (cavities) and contractions. The narrowest sections of contractions may be called windows. The connectivity and shape of the pores significantly affect the adsorption equilibrium as well as other phenomena that may occur in porous space, but usually the former characteristics are ignored by commonly used models (refs 17−22). For example, in the process of adsorption, the filling of some part of the cavities changes the situation in neighboring cavities via transformation of the cylindrical pore "without bottom" (the situation corresponding to cylindrical menisci) to pore "with bottom" (the situation corresponding to semispherical menisci). Similarly, formation of menisci in windows of empty cavity can provoke filling of this cavity, etc. This cooperative mechanism of pore filling may cause, for example, 30−50% deviations from values calculated by the simplified ideal model.[21,22]

Commonly used methods of description of complex pore space in real materials are based on a need to substitute a real morphology with the simple geometrical models that assume uniform pore shapes and the same effective size of pores. The model that represents a real porous network as a set of nonintersecting cylindrical pores of various diameters is the most common.[23] Moreover, the simplest algorithms ignore the mentioned cooperative effects. For example, the standard methods of pore size distribution calculations usually are based on the use of a desorption branch of adsorption isotherm,[23] where the cooperative effects caused by percolation processes are the most conspicuous.[17−22]

The discussion given above shows that the behavior of confined gas hydrates in mesopores under the field of surface forces has not yet been studied in detail. In addition, the data on gas hydrate dissociation considered above were obtained in a narrow range of thermodynamic parameters (e.g., the working pressure did not exceed 20 MPa).[6,10−14] The problem of the behavior of gas hydrate nanoparticles in a wide temperature and pressure range remains open. In this case, noticeable variations are possible for all of the parameters of eq 2. All of the problems considered above made this subject challenging in our viewpoint. In the present work, we report the results obtained during our studies of equilibrium dissociation conditions of confined methane hydrate in the pores of silica gels and nonmicroporous SBA-15[24] in a wide pressure range and at various water content in the mesopores of nanometer size.

Experimental Section

A standard set of silica gels, hydrophilic porous materials with a narrow distribution of mesopore sizes, KSK-1, KSK-2, KSS-3, KSS-4, KSM-5, and KSM-6p, commercially produced in the former Soviet Union was used. Additional experiments were performed on a nonmicroporous silicate mesoporous mesophase with the honeycomb structure Al-SBA-15 (atomic ratio Si/Al = 10), similar to that described previously in refs 24,25. This mesophase was used as a reference material with an independently defined shape and size of pores, which were calculated by the XRD/adsorption method.[26,27] In addition, all characteristics of Al-SBA-15 were calculated by the same methods which were used on silica gels.

All silica gels were calcined at 400 °C to oxidize organic impurities and were boiled in water for 24 h to hydroxylate the surface. Before use, the materials were repeatedly dried at 200 °C to remove the adsorbed water. Silica gels with a predetermined content of adsorbed water were obtained by keeping the samples over the standard KOH aqueous solutions. The attaining of equilibrium and the content of absorbed water were monitored by the mass change. In other experiments, water was added to a silica gel in some excess. The results of the measurements were the same as those obtained for the samples exposed to 100% water vapor.

The textural characteristics of all studied materials were determined by adsorption of nitrogen at 77 K using an ASAP-2400 instrument (Micromeritics). The errors of adsorption values and specific surface area measurements by ASAP-2400 are less than 1.56% as it follows from a special metrological study.[28] The samples were treated at 300 °C under vacuum before adsorption. All of the obtained isotherms had the hysteresis loops of capillary condensation of H1 or H2 type according to the IUPAC classification.[23] These isotherms were used for calculation of the specific values of the main texture parameters: the total surface area A_{BET} (BET method); the volume of micropores V_{micro}; the surface remaining after filling of micropores A_α (by a comparative method[26] analogous to the α_s method by Sing[23]); the total pore volume V_Σ (by saturation at $P/P_0 = 0.99$ relative pressure); and volumetric porosity $\epsilon = V_\Sigma\rho/(1 + V_\Sigma\rho)$, where ρ is the skeletal density which was assumed to be 2.2 g/cm^3. The average pore size was calculated by several methods. According to the first one, the values of $d_{BET} = 4V_\Sigma/A_{BET}$ were calculated. This method is the most commonly used for the systems with narrow pore size distributions. Next, the plots of pore volume distribution versus size were calculated by the well-known method of Barrett, Johner, and Halenda (BJH),[29] using the adsorption and desorption branches of the isotherms. From these plots, the values of $d_{max,ads}$ and $d_{max,des}$ were obtained that correspond to the maximums of the distributions for the adsorption and desorption branches, respectively. In addition, the average values of d_{ads} and d_{des}, defined as $4\sum V_i/\sum A_i$, where $\sum V_i$ and $\sum A_i$ are the cumulative values of pore volume and surface area, correspondingly, were calculated by the BJH method. Moreover, distribution according to the nonlocal DFT method in a model of cylindrical pores (ref 30) was calculated using the absorption isotherm branches, and d_{DFT} values were determined that corresponded to the distribution maximums. The results are reported in Table 1.

The temperatures of hydrate dissociation were measured by differential thermal analysis (DTA) under high pressures. The experimental apparatus was described in details elsewhere.[31] Samples of silica gel with adsorbed water were loaded into the DTA container with a volume of 0.05 mL. The container was hermetically assembled with a 6−8 mL stainless steel flask

TABLE 1: Texture Characteristics of the Adsorbents Used (Derived from the Isotherms of Nitrogen Adsorption at 77 K)

sample	A_{BET}[b] m^2/g	A_α[b] m^2/g	V_{micro}[b] cm^3/g	V_Σ[b] cm^3/g	ϵ[b]	pore diameter d (nm)[c] 1	2	3	4	5	6
KSK-1	316	316	0.0	0.890	0.66	11.3	12.6	10.4	3.9[a]	29.6 (11.8)	20.2 (9.3)
KSK-2	384	388	0.002	1.212	0.727	12.6	11.3	9.8	14.5	18.8 (9.2)	12.0 (2.7)
KSS-3	460	480	0.000	0.875	0.658	7.61	6.6	5.7	9.3	10.5 (6.3)	6.9 (1.3)
KSS-4	598	595	0.004	0.660	0.590	4.41	4.3	3.8	5.7	5.9 (4.1)	4.3 (1.0)
KSM-5	689	689	0.0	0.587	0.563	3.40	4.3	3.7	3.5		
KSM-6p	504	400	0.051	0.268	0.371	2.12	3.0	2.8	2.6		
Al-SBA-15	644	615	0.015	1.540	0.772	10.6	10.5	8.9	10.7	12.5 (3.5)	8.4 (1.1)

[a] This method is not appropriate for pores of this size. [b] A_{BET}, summary of the surface by the BET method; A_α, the surface remaining after filling the micropores; V_{micro}, the volume of micropores; V_Σ, total pore volume; ϵ, porosity. [c] The average pore diameters, d, are determined by the following methods: method 1, average diameter by BET; method 2, average diameter by BJH, the adsorption branch, ($d_{BJH}^{ads} = 4\sum V_i/\sum A_i$, where $\sum V_i$ and $\sum A_i$ are the summary values of the pore volume and surface, respectively, by the BJH method from the adsorption branch); method 3, average pore diameter by BJH, desorption branch ($d_{BJH}^{des} = 4\sum V_i/\sum A_i$); method 4, average diameter by DFT, adsorption branch; method 5, average diameter according to the pore size distribution maximum, adsorption branch; method 6, average diameter according to the pore size distribution maximum, desorption branch. For methods 5 and 6, the half-height width of the Gaussian peak is given in parentheses.

supplied with a movable piston and a back valve. After that, the flask was filled with the methane gas at pressures up to 2 MPa. A special technique was used for loading of the experimental cell with the silica gel and gas, which allowed one to avoid changes in the water content in the sample of silica gel. The assembled cell was placed into the zone of high hydrostatic pressure produced by compression of a silicon oil−hexane mixture. The pressure was transmitted into the cell by means of the piston. Temperatures of phase transformations were recorded in a course of heating the DTA cell at the moment of maximal difference of temperatures between standard thermocouple and thermocouple introduced into the container with sample. Typical experimental series included 7−15 independent cycles of freezing−seasoning/annealing of the sample to reach equilibrium−heating. Thermograms (sample temperature vs time and differential sample temperature vs time) were recorded at the last stage of the cycle. The appearance of peaks at the differential curve which corresponds to absorption of heat in the sample (will be referenced to below as thermal effects) evidenced a phase transformation taking place in the sample. In our case, thermal effects correspond to decomposition of all of the gas hydrate or some part of the gas hydrate in the sample. In the last case, several thermal effects corresponding to decomposition of different parts of gas hydrate in the sample occurred at the thermogram. The temperature of the sample measured at the moment of maximum peak at the differential curve corresponds to the decomposition temperature of the gas hydrate. In typical experiments, the decomposition points of the methane hydrates were measured with a chromel−alumel thermocouple in a standard DTA scheme with a heating rate of 1−2 °C/min. When calculating the K coefficients in eq 1, temperatures of hydrate dissociation under a given pressure were obtained by approximation of experimental data.

The thermocouple was calibrated using reference points or a reference thermometer. The systematic error in measurement of temperature by thermocouple did not exceed 0.2 °C. The pressure was measured with Bourdon manometers (up to 250 MPa), calibrated using a load-piston manometer. At higher pressures, a manganin manometer was used which was calibrated via the melting point of mercury. The systematic errors of pressure measurements did not exceed 1% of the measured pressure value for pressures above 200 MPa (manganin manometer, maximum error 10 MPa at pressure 1 GPa) and 0.5% of the measured pressure value for lower pressures (Bourdon gauge, maximum error 1 MPa at pressure 200 MPa). In our experiments, dissociation temperatures of gas hydrate were determined at a given pressure, and hence the maximum systematic error in determined dissociation temperatures includes

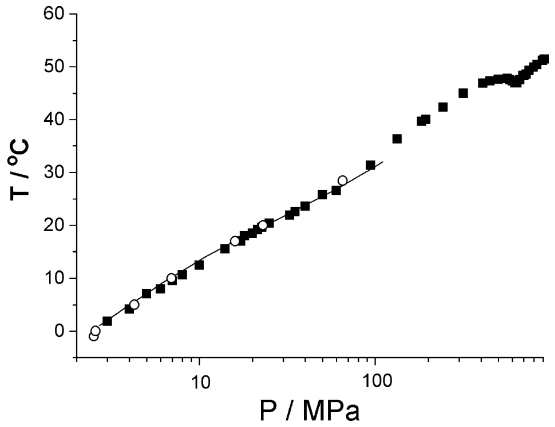

Figure 2. The results of dissociation of bulk methane hydrate (our data, ■) in comparison with the standard data in ref 5 (○) and the simulated dissociation curve calculated for bulk hydrate by the method of ref 9 (solid line). Errors in temperatures determined at a given pressure are less than the symbol size.

a typical error of temperature measurement by DTA method and an error in decomposition temperature caused by the uncertainty in pressure. This value in our experiments does not exceed ±0.3 °C. Correct operation of our experimental setup at pressures above 100 MPa was tested in a large series of DTA studies, and good agreement of our data with the data available from literature was observed in all cases (see, e.g., ref 31). To check the proper operation of the experimental setup at comparatively low pressures, the dissociation curve for bulk methane hydrate obtained on our equipment was compared to the standard data of ref 5 (Figure 2). In this case, the mean square deviation from the approximation curve was 0.2 °C (the value that includes all of the sources of accidental scattering of experimental points), which corresponds well to the typical values of 0.2−0.3 °C characteristic of our experiments on monovariant curves in double gas hydrate forming systems. The respective values were equal to 0.3 °C for KSK-1 and KSK-2, 0.5 °C for KSS-3, and 1 °C for KSS-4 silica gels. The reasons for a large scatter for the two latter cases are related to features of gas hydrate formation in mesopores of silica gel and will be discussed below.

Results and Discussion

The temperatures of methane hydrate dissociation for both bulk hydrate and hydrate in silica gels fully loaded with water are shown in Figure 3. One can see that the finer are the pores, the lower is the temperature of dissociation. However, in the

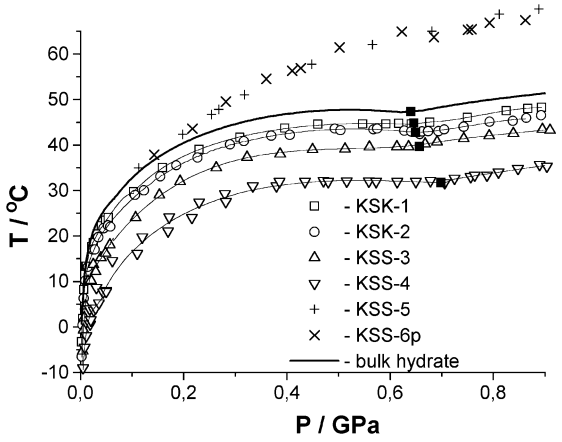

Figure 3. Dissociation curves of confined methane hydrate in silica gel pores. Results of the experiments where two thermal effects are at the same thermogram are omitted. For KSM-5 and KSM-6p silica gels, only "abnormal" thermal effects are shown (for comments, see the text). Quadrupole points are marked with big solid squares. Errors in temperatures determined at a given pressure are less than the symbol size.

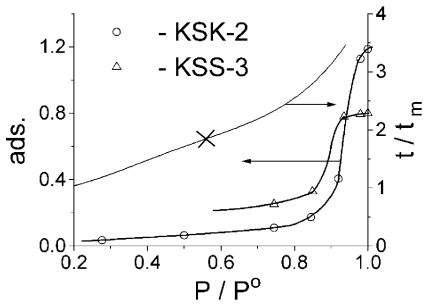

Figure 4. Fragments of water adsorption isotherms on KSK-2 and KSS-3 silica gels in coordinates: water adsorption ($g_{water}/g_{silicagel}$) versus relative water vapor pressure (P/P_0) (left axis). The plot marked by the cross is the dependence of the relative thickness, t/t_m, of the adsorbed water film on P/P_0, where t_m is the monolayer statistical thickness (about 0.115 nm), ref 36 (right axis).

case of KSM-5 and KSM-6 silica with the smallest pore size, there are "abnormal" effects with the temperature higher than that for bulk hydrate. In silica gels KSS-3 and KSS-4, a significant scatter of experimental points occurred, noticeably exceeding the instrumental errors; in some experiments, two slightly different in temperature thermal effects were observed below the dissociation temperature of bulk hydrate (these results are not shown in Figure 3 and will be discussed below). For the "normal" kind of effects, the behavior of $P-T$ dissociation curves for the hydrates in pores corresponds to that for bulk hydrate. A quadrupole point is distinctly noticeable for all curves in the pressure range of 0.6−0.8 GPa. At this point, a sharp turn of a dissociation curve and the appearance of its metastable prolongation are observed. This point corresponds to the phase transition of bulk hydrate of the cubic structure I to the hexagonal structure III[32] (structural types for gas hydrates were considered in details elsewhere[33,34]). This observation implies a correspondence between the structures of confined and bulk hydrates.

To clarify the effect of water content in silica gel on the decomposition temperature of the hydrate formed in pores of this silica gel, methane hydrate dissociation was studied for the silica gels partially filled with water. Water adsorption at ambient temperature over KSK-2 and KSS-3 samples (Figure 4) has been studied. These silica gels were selected for the experiments due to comparatively low scattering of experimental points (Figure 3) and sufficiently high sensitivity of $\Delta T(d)$ to small variations of d (see eq 1), which are characteristic for these samples. We assume that, at low relative pressures, adsorption of water vapor proceeds according to the mechanisms of mono- and multimolecular adsorption on the whole surface of silica gel. The thermodynamic activity of water in this layer is lower than that in the capillary condensate, and the adsorption layer can be considered as tightly bound to the surface. The rise of relative water vapor pressure results in the formation of capillary condensate in pores, with a corresponding steep increase in the adsorbed amount of water.

Hydrate dissociation was observed only for the samples with water content in a range of capillary condensation. This suggests that formation of methane hydrate in pores is possible only from the capillary condensate, whereas water of a tightly bound layer is not directly involved in the hydrate formation. Numerical experimental data that show the effect of the pore size on the melting temperature of individual liquids confined in pores[35] support this.

Studies of the thickness $t(P/P_0)$ of water film adsorbed over SiO_2 surface before capillary condensation are well known.[23,36−40] The values of $t(P/P_0)$ significantly depend on the degree of surface hydratation, presence of hydrophobic impurities, influence of capillary condensation that is not taken into account, etc.[41] The variations of $t(P/P_0)$ with changes of external parameters, such as temperature and pressure, are rather insignificant in the ranges of parameters concerned in this work. The surface of silica should be totally hydrated in a zone of methane hydrate formation. Thus, in Figure 4, we report the dependence of the relative thickness t/t_m, where t_m is the monolayer statistical thickness of the adsorbed water film on P/P_0 according to precise data by Zhdanov.[36] These measurements have been carried out over a hydrated surface of several species of quartz with the specific surface area of 0.2−0.5 m^2/g. In this case, full hydration and absence of capillary condensation was proved by total absence of any hysteresis and agreement of t/t_m versus (P/P_0). The thickness of the water layer, estimated from the t/t_m versus (P/P_0) plot, is 0.4−0.5 nm for KSK-2 and KSK-3 silica gels. The same values can be estimated from water adsorption isotherms over these silica gels, which are partially shown in Figure 4.

One can assume that the particles of hydrate in pores are surrounded with a layer of liquid water tightly bound to the surface of mineral particles (at least, at positive temperatures). The average pore size of silica gel in this case has to be diminished with the doubled thickness of this layer. Dissociation curves for the silica gels with capillary condensate are shown in Figure 5. If silica gels were not fully saturated with water, the temperatures of hydrate dissociation were as a rule somewhat (1−2 °C) lower than those for the corresponding curve of silica gel totally saturated with water. This displacement could be caused by the fact that, during capillary condensation, the smaller pores were filled with liquid first, and, thus, the hydrate was formed in the smaller pores; hence, the average pore size for the hydrate formation would be diminished. Our data show a relatively low total effect of these factors on the dissociation temperature of the hydrate confined in pores.

In general, the dissociation temperature of confined gas hydrate in silica gel mesopores depends on the value of the apparent size of the hydrate particles, specific interfacial water−hydrate energy, γ_{hw}, the shape coefficient a characteristic of hydrate particles, and, perhaps, the existence of the meniscus and its curvature radii on the gas−water interface. The existence of the tightly bound water layer decreases the apparent size

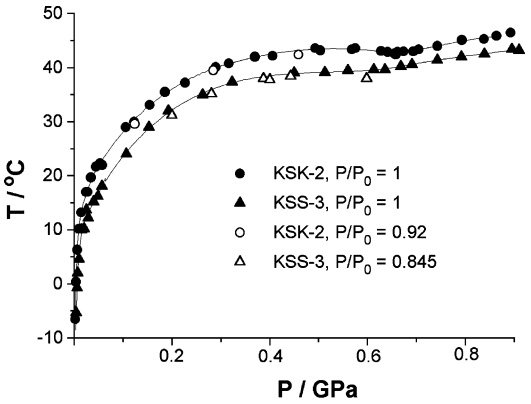

Figure 5. Dissociation temperatures of confined hydrates in KSK-2 and KSS-3 with different degrees of pore filling with water. P/P_0 represents the relative water vapor pressure at which silica gel was saturated with water. The minimum water contents at which hydrate formation was observed are shown. Errors in temperatures determined at given pressure are less than the symbol size.

value.[42] Now, let us consider the effect of the listed parameters on the dissociation temperature of the confined hydrate.

Let us consider allocation of solid hydrate particles in the interlinked porous space of a material with silika gel-type texture discussed above (Figure 1a). The shape of hydrate particles may replicate a host space of pores and cannot be considered in the terms of simple geometrical shapes such as an ideal sphere or cylinder. A single hydrate particle can be located in one or several neighbor cages and may have a globular, elongated, or more complex (e.g., fractal) shape. One should consider several aspects of hydrate formation in the mesopores. Formation of comparatively small hydrate particles near the external surface of silica particles (Figure 1b) is the most probable situation for the short-time laboratory experiments. The formation of large clusters such as that shown in Figure 1c is possible in natural conditions, where slow diffusion of gas molecules through the liquid component of the intraporous media is possible during dozens and hundreds of years. Additionally, the existence of the firmly bounded liquidlike film of water between the surfaces of silica and hydrate particles is probable by analogy with the situation observed for ice particles grown in mesopores.[35,42] The surface curvature K_m in the considered case cannot be calculated by using such simple determinations of principal radii of curvature values (eq 3).[43,44] In this case, the coefficient a in eq 2 should be considered as a coefficient depending on the hydrate particle shape. As a "first iteration", we can consider this coefficient to correspond to the "apparent shape" both of hydrate particles and of pores, simultaneously. One can assume that the values of this coefficient can vary between 4 and 2 that are characteristic for globular (quasi-spherical) and elongated (quasi-cylindrical) particles, respectively. The apparent size of hydrate particles can be expressed via the ratio of the volume occupied by hydrate particles to the total hydrate/silica interface surface. As an alternative, one can express it as a mean size of cavities confining hydrate particles for estimations. It should be emphasized that the apparent size of hydrate particles generally does not correspond to the size determined from simplified models. In addition, values of the shape coefficient a and the apparent size of the hydrate particles are interrelated (see eqs 1 and 2). At present, no methods of pore structure characterization are known which can correctly determine all morphological and topological characteristics of porous space. High-resolution X-ray or electron microscopy, thermoporometry, ^{129}Xe NMR, etc. (refs 45,46) are not capable of solving this complicated problem. It is particularly interesting that the traditional absorption method is often used for calibration of mentioned methods.[46] The only way to independently determine the shape coefficient a and the apparent size of the hydrate particles is in using the porous material with a simple and unambiguously determined shape and size of pores. At present, such porous materials exist, for example, silicate mesoporous mesophases of type MCM-41 and SBA-15.[24−27,47,48] The porous structure of these mesophases is similar to honeycomb and is formed by parallel pores of uniform diameter d, which in the case of nonmicroporous mesophases can be accurately calculated from the combination of X-ray and adsorption data as $d = a_0\epsilon^{1/2}$ (where a_0 is the parameter of hexagonal framework of pores, and ϵ is the porosity).[25−27] The structural regularities and simple pore shape of these mesoporous materials allow their application as reference materials for the verification of phase transformation temperature shifts in pores with complex shape. We used SBA-15 silica as the reference material in this work. The results of comparing pore sizes for silica gels and this reference are discussed below.

The available γ_{hw} values for the water−methane hydrate interface obtained or taken a priori in the literature do not decline significantly from the γ_{hw} value for the water−ice interface.[11−14] Assuming that both the hydrate and the ice frameworks are built up from similar particles with similar characteristics of hydrogen bonds, one can expect similar interfacial energies. Critical review of γ_{hw} values available for the water−ice and water−hydrate interfaces (refs 7−14 and references within) allows the conclusion that the most reliable value so far of γ_{hw} for the water−methane hydrate boundary is 0.029 J/m^2.

The method of differential thermal analysis used in this work gives a maximum thermal effect at the temperature of hydrate dissociation in the predominant pores of the sample: the volume portion of the hydrate in these pores is maximum and, hence, causes the maximal heat absorption. The monitored temperature of hydrate dissociation corresponds to the hydrate dissociation in such pores, and the scatter of pore size causes just a broadening of the differential peak. Finally, taking into account the geometrical reasons, the main mass of hydrate particles has to occupy the wide parts ("cavities") in the labyrinth of pores, and, hence, for the evaluation of the apparent size of the hydrate particle, the mean size has to be determined using the adsorption branches of hysteresis ranges on the nitrogen adsorption isotherms at 77 K. So, we believe the pore diameters determined by method 5 (but not by commonly used methods 1−3; see Table 1 and the Experimental Section) are the most adequate for quantitative description of the confinement effect in silica gels and similar materials.

As it follows from eqs 1 and 2, the shape of the particles of a confined hydrate affects the dissociation temperature: with the same value of γ_{hw}, ΔT has to differ two-fold for ideal spherical and ideal cylindrical particles. The real shapes of particles of confined hydrate differ from the ideal spherical or cylindrical shape (see Introduction and discussion above), but one should expect that the shape coefficient a for these particles lies between the values characteristic of spherical and cylindrical shapes. The shape coefficient values characteristic of real particles may depend on the shape and size of the confining pores and the conditions of sample preparation, and hence decomposition temperatures of confined hydrate may scatter to some extent. To check this hypothesis, we calculated the dissociation curves of methane hydrate in porous media under the pressures up to 100 MPa (the upper limit of the model validity), along with the dissociation curve of bulk methane hydrate (shown in Figure 2). The calculations have been

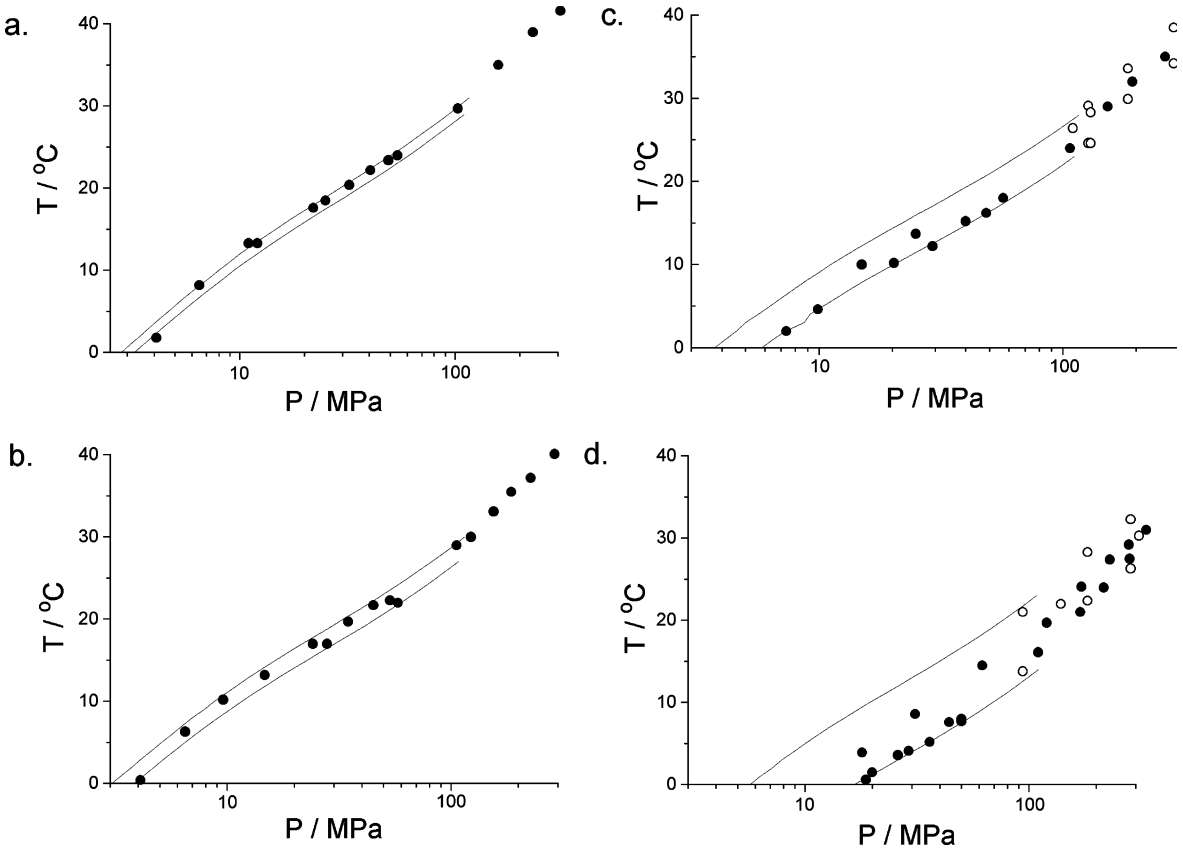

Figure 6. Experimental results of dissociation temperatures of confined methane hydrate in the following: (a) KSK-1 ($d = 29.6$ nm), (b) KSK-2 ($d = 18.8$ nm), KSS-3 ($d = 10.5$ nm), and KSS-4 ($d = 5.9$ nm) in comparison with the curves simulated for hydrate particles of 28.6, 17.8, 9.5, and 4.9 nm, respectively (the size of hydrate particles is equal to a mean pore diameter diminished by the thickness of tightly bound water layer). The upper and lower curves are calculated with the assumption of elongated and globular particle shapes of the hydrate, respectively. Open symbols denote the experimental series with two thermal effects on the thermograms. Errors in temperatures determined at a given pressure are less than the symbol size.

performed by the method suggested in ref 9. For these calculations, the typical pore size determined by method 5 (Table 1) diminished by the doubled thickness of the tightly bound water layer (2×0.5 nm) was accepted. The value of specific interfacial energy on the water−hydrate interface was assumed to be 0.029 J/m^2. The probable occurrence of the meniscus on the gas−water interface was not taken into account; the boundary was supposed to occur outside of the pores. Calculations were performed for globular (quasi-spherical, $a = 4$) and elongated (quasi-cylindrical, $a = 2$) particle shapes of hydrate. Simulated curves are shown in Figure 6, in comparison with the experimental data. The results of the experiments in which two thermal effects were detected are shown by open symbols in Figure 6. In all cases, experimental points for a silica gel fit the range between the simulated curves for the quasi-spherical and quasi-cylindrical hydrate particles. For the silica gels KSK-1 and KSK-2, experimental points lie closer to the simulated curve for the quasi-cylindrical hydrate particles (upper curve), whereas for silica gels KSS-3 and KSS-4, the points predominantly lay on the lower curve calculated for the quasi-spherical particles, while a significant scatter of the points is observed between the upper and lower curves. In the cases where two thermal effects were observed for silica gels KSS-3 and KSS-4 (Figure 6c and 6d), the sets of effects at upper and lower temperatures corresponded to the simulated curves for quasi-cylindrical and quasi-spherical particles, respectively. The obtained results imply that the particle shape of the confined hydrate in silica gel pores appears to significantly depend on the pore size and may differ in different experiments with the same samples of mesoporous material. A probable explanation of this observation may be related to the different shapes of the particles of the confined hydrate. In large pores, it may be closer to the elongated shape due to coalescence of hydrate particles in neighboring cavities. In the fine pores, the size of the windows between cavities does not allow coalescence of hydrate particles; the shape of hydrate particles appears to be closer to globular. Indubitably, the pore shape of the dispersion medium (silica gel, porous glass) can affect the shape of the hydrate particles enclosed, and experimental results can be different for samples with the same typical pore size. The scatter of experimental points and occurrence of two thermal effects observed in silica gels KSS-3 and KSS-4 can be assigned to the presence of hydrate particles of different shape that decompose at different temperatures, respectively. This effect can be caused either by the presence of pores of different shape in the sample, in the case of an equilibrium system, or, in the case of a nonequilibrium system, by the formation of quasi-spherical particles within the elongated pores, when their further development is halted by their blocking in the pores. On the other hand, a fairly good agreement between the calculated and experimental data provides, in our opinion, an essential argument for the validity of the calculation method proposed in ref 9 for the equilibrium curves of gas hydrate in pores, as well as for our suggestions concerning the techniques for selection of pore size and the occurrence of the water layer not taking part in hydrate formation. One more argument in support of considerations given above is provided by the results of our experiments on the mesoporous Al-SBA-15 silica gel with cylindrical pores. The structural characteristics of Al-SBA-

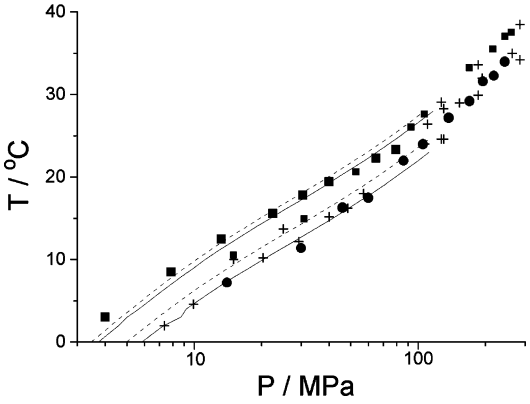

Figure 7. Experimental results of dissociation temperatures of confined methane hydrate in the cylindrical pores of Al-SBA-15 (■) in comparison with the results for KSS-3 (crosses) and simulated results for quasi-spherical (lower curves) and quasi-cylindrical (upper curves) hydrate particles with diameters of 11.5 nm (dashed lines) and 9.5 nm (solid lines). Errors in temperatures determined at a given pressure are less than the symbol size.

15 additionally were calculated by the XRD/adsorption method[26,27] using the mesophase porosity $\epsilon = 0.654$ from nitrogen adsorption and the hexagonal cell parameter $a_0 = 15.2$ nm from XRD. Accordingly, the mesopore diameter $d_{Me} = a_0\epsilon^{1/2} = 10.67$ nm. (The "external" surface area remained after mesopore filling, $A_{ext} = 548$ m^2/g, and the total surface area, $A_\Sigma = 739$ m^2/g, and mesopore volume, $V_{Me} = 0.86$ cm^3/g, were calculated.)

The result of the independent method, ~10.7 nm, was in quite good agreement with the results of methods 1, 2, and 4 (Table 1) and was only slightly lower than the average diameter obtained by method 5 (12.5 nm). On the thermograms of the confined hydrate in this mesoporous sample, two thermal effects were observed, their positions fairly corresponding to the simulated curves for the elongated and globular shapes of hydrate particles with both determined pore diameters (Figure 7). Experimental points on KSS-3 with a pore diameter of 10.5 (method 5) also fit the data obtained on Al-SBA-15 (Figure 7). We will continue our efforts with this type of mesoporous media.

To compare our data with the results of refs 11−14, we used eq 1 for processing of our experimental curves. Temperatures of methane hydrate dissociation in silica gels KSK-1, KSK-2, KSS-3, and KSS-4 at pressures of 10, 25, 50, 100, 200, 400, 600, and 800 MPa have been determined by interpolation of experimental points (see Experimental Section). Only those experiments were taken into account in which a single thermal effect per termogram occurred. In our opinion, it is appropriate to discuss the results of this work in terms of the K coefficient value, as it is directly related to the decrease of the dissociation temperature of a hydrate within the pores of a given size. The values of K calculated from our data for the pore diameters determined by methods 1, 2, and 5, taking into account the tightly bound water layer not participating in hydrate formation (pore size was diminished by the thickness of two layers of 0.5 nm each), are given in Table 2. A typical example of a correlation plot is given in Figure 8. The results based on the pore sizes calculated by methods 1 and 2 actually cannot be discerned. Table 2 shows that the relationship between $\Delta T/T_{bulk}$ and $1/d$ remains practically linear, despite the change of the typical particle shape in pores (as discussed above). The apparent value of K depends on the method of pore size determination. Conventionally used methods 1 and 2 give K values close to those obtained in refs 12, 14, and method 5 (which we take as the most reliable) gives significantly higher K values. Unfortunately, the lack of detailed information on the methods used in refs 12, 14 for pore size determination renders further discussion of the problem impossible.

TABLE 2: K and A Parameters of the $\Delta T/T = A - K(1/d)$ Correlation Equation at Different Pressures, Calculated by Different Methods of Pore Size Determination from Our Data on the Dissociation Temperature Decrease for Methane Hydrate in KSK-1, KSK-2, KSS-3, and KSS-4 Silica Gels

	method 5			methods 2,3		
P/MPa	K (/nm)	A^c*10^3	R^c	K (/nm)	A^c*10^3	R^c
10[a]	0.29 ± 0.04	6 ± 5	−0.9988	0.22 ± 0.04	13 ± 8	−0.9983
25[a]	0.30 ± 0.02	2 ± 2	−0.9998	0.22 ± 0.06	10 ± 11	−0.9960
50[a]	0.29 ± 0.04	1 ± 5	−0.9990	0.22 ± 0.04	8 ± 8	−0.9981
100[a]	0.26 ± 0.04	1 ± 5	−0.9987	0.19 ± 0.04	7 ± 8	−0.9972
200[a]	0.24 ± 0.02	1 ± 3	−0.9996	0.18 ± 0.03	5 ± 6	−0.9985
400[a]	0.23 ± 0.02	1 ± 3	−0.9995	0.17 ± 0.03	5 ± 5	−0.9988
600[a]	0.23 ± 0.01	0 ± 1	−0.9999	0.17 ± 0.04	6 ± 7	−0.9972
800[b]	0.24 ± 0.05	1 ± 6	−0.9979	0.18 ± 0.07	5 ± 13	−0.9807

[a] Hydrate of cubic structure I. [b] Hydrate of hexagonal structure III. [c] A is the argument of the regression equation; according to eq 1, it should not differ from 0. R is the linear regression coefficient.

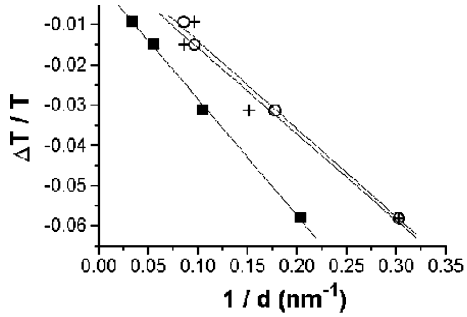

Figure 8. A typical $\Delta T/T_{bulk}$ versus $1/d$ correlation plot (at 50 MPa pressure) for different methods of pore size determination. Squares represent method 5, circles represent method 2, and crosses represent method 1.

The second essential conclusion from the data of Table 2 follows from a weak dependence of K on pressure. The values of K obtained under various pressures differ very slightly, including the point at 800 MPa that corresponds to dissociation of the hexagonal structure III hydrate. The obtained divergence of K values in the pressure range below 100 MPa just slightly exceeds the experimental scatter and cannot be considered as reliable. On the whole, the weak sensitivity of dissociation temperature decrease toward the pressure applied can be concluded. Within the approach used for the derivation of eq 2, the changes of the values of γ_{hw} and the product of hydrate density by the dissociation heat, $\rho_h L_h$, compensate each other, being, respectively, parts of the numerator and the denominator in eq 2.

Thermal effects referred to above as "abnormal" were observed for KSM-5 and KSM-6p silica gels with the smallest pore sizes among all used samples. These thermal effects were not reproducible enough, their causes remaining obscure. At the same time, the values of these effects and the discrepancy between their temperatures and dissociation temperatures of other phases present in the system exclude them from the possible experimental errors. Our observation gives the first example of an increase of decomposition temperatures of confined gas hydrate in mesoporous silica. So far, we cannot interpret unambiguously the "abnormal" effects, and additional work is necessary to understand the physical reasons of their appearance.

Conclusions

According to our study of the equilibrium dissociation of methane hydrates in silica gel pores, we would like to summarize several peculiarities of these systems. It is shown that the most adequate method of determination of the apparent size of pores in silica gels (and similar compounds) is by the determination of the size of pores most abundant in the sample (referred to above as method 5). This allows reliable studies of the relationships between the pore size and the dissociation temperature of confined gas hydrates in these media. The obtained experimental data support the possibility of different shapes of hydrate particles existing in the pores of silica gel and the influence of this effect on the dissociation temperature of confined hydrate in pores. In this Article, we referred to these shapes as globular (quasi-spherical) and elongated (quasi-cylindrical). A decrease of the dissociation temperature of methane hydrate in mesoporous silica gel was experimentally shown to be weakly dependent on the pressure. Our data show that hydrate can be formed in pores only from the capillary condensate, whereas the water layers tightly bound to the surface do not take part in its formation. The obtained experimental data show the possibility of stabilization of hydrates in silica gel pores of less than 5 nm, as compared to the bulk hydrate.

Acknowledgment. This work was supported by a grant of Presidium SB RAS N^o 147, RFBR grants 03-03-32020a and 04-03-32578a, and grant 2120.2003.3 from the Russian Ministry of Science. A.Yu.M. thanks the "Russian Science Support Foundation" for financial support.

References and Notes

(1) Kvenvolden, K. A. *Ann. N.Y. Acad. Sci.* **2000**, *912*, 17.
(2) *Initial Reports of the Deep Sea Drilling Project*, 1982, Leg 67; 1985, Leg 84.
(3) Brooks, J. M.; Kcnnicutt, M. C.; Fay, R. R.; McDonald, T. J. *Science* **1984**, *225*, 409.
(4) Kvenvolden, K. A.; McDonald, T. J. *Initial Reports of the Deep Sea Drilling Project* 1985, Leg 84, p 667.
(5) Istomin, V. A.; Yakushev, V. S. *Gazovye gidraty v prirodnyh usloviyah (Gas hydrates in nature)*; Nedra: Moskow, 1992 (in Russian).
(6) Handa, Y. P.; Stupin, D. *J. Phys. Chem.* **1992**, *96*, 8599.
(7) Clennell, M. B.; Hovland, M.; Booth, J. S.; Henry, P.; Winters, W. J. *J. Geophys. Res. B* **1999**, *104(B10)*, 22985.
(8) Henry, P.; Thomas, M.; Clennell, M. B. *J. Geophys. Res. B* **1999**, *104(B10)*, 23005.
(9) Melnikov, V. P.; Nesterov, A. N. *Earth's Cryosphere (Special Issue)* **2003**, 76.
(10) Smith, D. H.; Wilder, J. W.; Seshadri, K.; Zhang, W. *Proceedings of the Fourth International Conference on Gas Hydrates*; Yokohama, May 19−23, 2002; p 295.
(11) Uchida, T.; Ebinuma, T.; Ishizaki, T. *J. Phys. Chem. B* **1999**, *103*, 3659.
(12) Uchida, T.; Ebinuma, T.; Takeya, S.; Nagao, J.; Narita, H. *J. Phys. Chem. B* **2002**, *106*, 820.
(13) Anderson, R.; Liamedo, M.; Tohidi, B.; Burgass, R. W. *J. Phys. Chem. B* **2003**, *107*, 3500.
(14) Anderson, R.; Liamedo, M.; Tohidi, B.; Burgass, R. W. *J. Phys. Chem. B* **2003**, *107*, 3507.
(15) van der Waals, J.; Platteeuw, J. C. *Adv. Chem. Phys.* **1957**, *2*, 1.
(16) In modern literature this equation is known as Gibbs−Thomson equation due to its similarity to a more famous fundamental equation of capillarity known as the Kelvin (William Thomson lord Kelvin) equation. But as C. Faivre et al. mention in *Eur. Phys. J. B* **1999**, *7*, 19, the possibility of a variation of the melting temperature from size was first mentioned (without equation) by J. J. Thomson in *Application of Dynamics*, London, 1888), and equation (1) was for the first time published by E. Rie, *Z. Physik. Chem.* **1923**, *104*, 354.
(17) Amyx, J. W.; Bass, D. M.; Whiting, R. L. *Petroleum Reservoir Engineering*; McGraw-Hill Book Company, Inc.: New York−Toronto−London, 1960.
(18) Sahimi, M. *Application of Percolation Theory*; Taylor & Francis: London, 1994.
(19) Zhdanov, V. P. *Adv. Catal.* **1993**, *39*, 1.
(20) Efremov, D. K.; Fenelonov, V. B. *Pure Appl. Chem*. **1993**, *65*, 2209.
(21) Efremov, D. K.; Fenelnov, V. B. *Kinet. Catal.* **1993**, *34*, 555.
(22) Davis, G. M.; Seaton, N. A. *Carbon* **1998**, *36*, 1473.
(23) Gregg, S. J.; Sing, K. S. W. *Adsorption, Surface Area and Porosity*, 2nd ed.; Academic Press: London, 1982.
(24) Mel'gunov, M. S.; Mel'gunova, E. A.; Shmakov, A. N.; Zaikovskii, V. I. In *Nanotechnology in Mesostructured Materials. Studies in Surface Science and Catalysis*; Park, S.-E., Ryoo, R., Ahn, Wh.-S., Wee Lee, Ch., Eds.; Elsevier: New York, 2003; Vol. 146, p 543.
(25) Fenelonov, V. B.; Derevyankin, A. Yu.; Kirik, S. D.; Solovyov, L. A.; Schmakov, A. N.; Bonaret, J. L.; Gedeon, A.; Romannikov, V. N. *Microporous Mesoporous Mater.* **2001**, *44*−*45*, 33.
(26) Fenelonov, V. B.; Romannikov, V. N.; Derevyankin, A. Yu. *Microporous Mesoporous Mater.* **1999**, *28*, 57.
(27) Kruck, M.; Jarroniec, M.; Sayari, A. *Langmuir* **1997**, *13*, 6267.
(28) Fenelonov, V. B.; Okkel, L. G.; Slyudkina, N. S.; Malygina, T. M. *Instrum. Exp. Tech*. **1977**, *40*, 559.
(29) Barrett, E. P.; Joyner, L. G.; Halenda, P. H. *J. Am. Chem. Soc.* **1951**, *73*, 373.
(30) Ravikovitch, P. I.; Neimark, A. V. *Colloids Surf., A* **2001**, *187*, 11.
(31) Dyadin, Yu. A.; Larionov, E. G.; Mirinskij, D. S.; Mikina, T. V.; Aladko, E. Ya.; Starostina, L. I. *J. Inclusion Phenom*. **1997**, *28*, 271
(32) Loveday, J. S.; Nelmes, R. J.; Guthrie, M. e. a. *Nature* **2001**, *410*, 661.
(33) Jeffrej, G. A. In *Comprehensive Supramolecular Chemistry*; Atwood, J. L., Davies, J. E. D., MacNicol, Vogtle, F., Eds.; Oxford Elsevier Science Ltd.: New York, 1996; Vol. 6, p 757.
(34) Dyadin, Yu. A.; Bondaryuk, I. V.; Zhurko, F. V. In *Inclusion Compounds*; Atwood, J. L., Davies, J. E. D., MacNicol, Eds.; Oxford University Press: Oxford, 1991; Vol. 5, p 213.
(35) Christenson, H. K. *J. Phys.: Condens. Matter* **2001**, *13*, R95.
(36) Zhdanov, S. P. *Dokl. Acad. Nauk SSSR* **1958**, *120*, 103 (in Russian).
(37) Hagumassy, J.; Brunauer, S.; Mikhail, R. Sh. *J. Colloid Interface Sci.* **1969**, *29*, 485.
(38) Morimoto, T.; Nagao, M.; Imai, Ju. *Bull. Chem. Soc. Jpn.* **1971**, *44*, 1285.
(39) Partuko, S.; Rouquerol, F.; Rouquerol, J. *J. Colloid Interface Sci.* **1979**, *68*, 21.
(40) Fenelonov, V. B.; Okkel, L. G. *React. Kinet. Catal. Lett.* **1994**, *52*, 331.
(41) Kiselev, A. V. *Intermolecular Interactions in Adsorption and Chromatography*; Vysshaya Shkola: Moskow, 1986.
(42) Gelb, L. D.; Gubbins, K. E.; Radhakrishnan, R.; Sliwinska-Bartkowiak, M. *Rep. Prog. Phys.* **1999**, *62*, 1573.
(43) DeHoff, R. T. In *Quantitative Microscopy*; DeHoff, R. T., Rhines, F. N., Eds.; McGraw-Hill Book Co.: New York, 1968; p 291.
(44) Anderson, S.; Hyde, S. T.; Larsson, K.; Lidin, S. *Chem. Rev.* **1988**, *88*, 221.
(45) *Physical Adsorption: Experiment, Theory and Application*; Fraissard, J., Conner, C. W., Eds.; Kluwer Academic Publ.: Dordrecht, 1997.
(46) *Characterization of Porous Solids, I, II, III, IV, Proceeding IUPAC Symp.*; Elsevier: Amsterdam, 1987; 1990; 1993; 1997.
(47) Kresge, C. T.; Leonowicz, M. E.; Roth, W. J.; Vartuli, J. C.; Beck, J. C. *Nature* **1992**, *359*, 710.
(48) Zhao, D.; Huo, Q.; Feng, J.; Chmelka, B. F.; Stucky, G. D. *J. Am. Chem. Soc*. **1998**, *120*, 6024.